Atmos. Chem. Phys., 9, 5921–5932, 2009
www.atmos-chem-phys.net/9/5921/2009/

Atmospheric Chemistry and Physics

Measurements of particle masses of inorganic salt particles for calibration of cloud condensation nuclei counters

M. Kuwata[1,*] **and Y. Kondo**[1]

[1]Research Center for Advanced Science and Technology, the University of Tokyo, Tokyo, Japan
[*]currently at: School of Engineering and Applied Sciences, Harvard University, Cambridge, MA, USA

Received: 7 January 2009 – Published in Atmos. Chem. Phys. Discuss.: 24 February 2009
Revised: 27 July 2009 – Accepted: 1 August 2009 – Published: 19 August 2009

Abstract. We measured the mobility equivalent critical dry diameter for cloud condensation nuclei (CCN) activation (d_{c_me}) and the particle mass of size-selected $(NH_4)_2SO_4$ and NaCl particles to calibrate a CCN counter (CCNC) precisely. The CCNC was operated downstream of a differential mobility analyzer (DMA) for the measurement of d_{c_me}. The particle mass was measured using an aerosol particle mass analyzer (APM) operated downstream of the DMA. The measurement of particle mass was conducted for 50–150-nm particles. Effective densities (ρ_{eff}) of $(NH_4)_2SO_4$ particles were 1.67–1.75 g cm^{-3}, which correspond to dynamic shape factors (χ) of 1.01–1.04. This shows that $(NH_4)_2SO_4$ particles are not completely spherical. In the case of NaCl particles, ρ_{eff} was 1.75–1.99 g cm^{-3} and χ was 1.05–1.14, demonstrating that the particle shape was non-spherical. Using these experimental data, the volume equivalent critical dry diameter (d_{c_ve}) was calculated, and it was used as an input parameter for calculations of critical supersaturation (S). Several thermodynamics models were used for the calculation of water activity. When the Pitzer model was employed for the calculations, the critical S calculated for $(NH_4)_2SO_4$ and NaCl agreed to well within the uncertainty of 2% (relative). This result demonstrates that the use of the Pitzer model for the calibration of CCNCs gives the most accurate value of S.

1 Introduction

The number concentration of cloud condensation nuclei (CCN) is an important parameter for cloud microphysics. The number concentration and size distribution of cloud droplets are affected by changes in the CCN number concentration. Consequently, CCN number concentration is indirectly related to radiative forcing and the hydrological cycle. Thus, it is important to measure the CCN number concentration and CCN activity of atmospheric particles precisely (Twomey, 1974; Lohmann and Feichter, 2005, and references therein).

CCN number concentration is measured using a CCN counter (CCNC). Several types of CCNCs have been developed (McMurry, 2000; Nenes et al., 2001; Roberts and Nenes, 2005). In most CCNCs, supersaturated conditions are produced by creating a temperature difference on wetted walls. CCN-active particles grow to large droplets in the artificial supersaturated environment. The number of droplets is then counted using an optical particle counter (OPC) (e.g., Stratmann et al., 2004; Roberts and Nenes, 2005) or a charge coupled device (CCD) camera (Otto et al., 2002). The most important parameter in CCN measurement is the precise value of the supersaturation (S) inside the instrument, which ensures compatibility with other studies (Seinfeld and Pandis, 2006).

S inside a CCNC can be calculated theoretically (e.g., Nenes et al., 2001; Stratmann et al., 2004; Roberts and Nenes, 2005). These theoretical studies are indispensable for developing CCNCs. However, theoretical results are not sufficient for practical observations and experiments as the ideal instrument does not exist and instrumental conditions can change with time. Therefore, routine calibrations are required for the operation of CCNCs (e.g., Rose et al., 2008). Unfortunately, there are no instruments that can measure S directly; thus, we have to choose an alternative method for calibration. In most CCN studies, the critical dry diameters (the threshold diameters for CCN activation, d_c) of laboratory-generated particles are measured using a CCNC connected to a differential mobility analyzer (DMA) in tandem to calibrate the instruments. Then, the critical S values corresponding to the observed d_c values are calculated using Köhler theory. $(NH_4)_2SO_4$ is the most frequently used compound for calibration (e.g., Kumar et al., 2003; VanReken et

Correspondence to: M. Kuwata
(kuwata@atmos.rcast.u-tokyo.ac.jp)

al., 2005), and some studies also use NaCl particles (Rissman et al., 2007; Shilling et al., 2007; Rose et al., 2008). However, the critical S of $(NH_4)_2SO_4$ particles is strongly dependent on thermodynamics models (Kreidenweis et al., 2005), and the magnitude of the variation is large enough to change the interpretation of the observation results (e.g., Mochida et al., 2006). In the case of NaCl, the differences between thermodynamics models are not as significant as those of $(NH_4)_2SO_4$, and there is an excellent thermodynamics model that is based on the various experimental data (Archer, 1992). However, it is difficult to estimate the critical S of a DMA-selected NaCl particle because of its non-spherical shape (Kelly and McMurry, 1992; Zelenyuk et al., 2006a). In previous studies, S values calculated using the two different compounds did not always agree, and the magnitude of the difference was up to 10% (relative) (e.g., Shilling et al., 2007). These discrepancies were possibly caused by the uncertainties described above. Rose et al. (2008) have suggested that the shape factor of NaCl particles varies between 1.0 and 1.08 based on measurements of the CCN activity of NaCl particles. We have measured this quantity more accurately using a more direct method.

In this study, we measured the masses of $(NH_4)_2SO_4$ and NaCl particles generated for the calibration of a CCNC using an aerosol particle mass analyzer (APM). The APM can select particles according to their mass by virtue of the balance between electrostatic and centrifugal forces (Ehara et al., 1996). Thus, the combination of a DMA and an APM (DMA-APM system) enables us to measure the mass of DMA-selected particles, and we can obtain parameters related to particle morphology such as χ (e.g., Park et al., 2004). Then, S values inside the CCNC were calculated using the measured d_c, particle mass, and several thermodynamics models. The calculated S values are compared to investigate the consistency of the experimental results of $(NH_4)_2SO_4$ and NaCl particles.

2 Theoretical background

2.1 The relationship of d_{me} and d_{ve}

In this section, we summarize the relationship between mobility diameter (d_{me}) and volume equivalent diameter (d_{ve}), because the conversion of d_{me} to d_{ve} is needed to prepare an input parameter for calculations based on Köhler theory (Sect. 2.2). For spherical particles, d_{me} is equal to d_{ve}. However, particles are not always spherical. Using the effective density (ρ_{eff}), d_{me} is related with d_{ve} by the following equation (DeCarlo et al., 2004):

$$m_p = \frac{\pi}{6}\rho_m d_{ve}^3 = \frac{\pi}{6}\rho_{\text{eff}} d_{me}^3 \tag{1}$$

or

$$d_{ve} = \sqrt[3]{\frac{\rho_{\text{eff}}}{\rho_m}} d_{me} \tag{2}$$

where m_p is particle mass, and ρ_m is the material density. In the DMA-APM system, d_{me} is known as it is prescribed by the DMA, and m_p can be measured using the APM. Thus, if we apply this experimental system to particles composed of single compounds, we can obtain the conversion factor $\left(\sqrt[3]{\frac{\rho_{\text{eff}}}{\rho_m}}\right)$ easily, as ρ_m is a known parameter.

d_{ve} and d_{me} can also be related by χ, which is defined as the ratio of the drag force acting on spherical particles with diameters of d_{ve} and d_{me}. Under the equilibrium sphere approximation (ESA) (Dahneke, 1973), χ is defined by the following equation (Kasper, 1982):

$$\chi = \frac{Z_p(d_{ve})}{Z_p(d_{me})} = \frac{C_c(d_{ve})}{d_{ve}} \frac{d_{me}}{C_c(d_{me})} \tag{3}$$

where Z_p is the electrical mobility, and the slip correction factor (C_c) can be calculated from the following equation (Allen and Raabe, 1985):

$$C_c = 1 + \frac{2\lambda}{d_p}\left(1.142 + 0.558\exp\left(\frac{\frac{-0.009}{2\lambda}}{d_p}\right)\right) \tag{4}$$

where λ is mean free path of air. Although ESA is a good approximation for slightly non-spherical particles and it is useful to calculate χ from experimental results, it is not always appropriate to use ESA for studies of χ in the transition regime (χ_t), especially for particles that are highly non-spherical (Dahneke, 1973). For this purpose, the adjusted sphere approximation (ASA) was introduced (Dahneke, 1973). Using ASA, χ_t can be written as follows (DeCarlo et al., 2004):

$$\chi_t = \chi_c \frac{C_c(d_{ve})}{C_c\left(\frac{\chi_f}{\chi_c} d_{ve}\right)} \tag{5}$$

where, χ_f and χ_c denote χ in the free molecular regime and continuous regime, respectively.

2.2 Köhler theory

The water activity of an aqueous solution (a_w) is equal to the saturation ratio of water vapor (Robinson and Stokes, 2002)

$$\frac{p_w}{p_w^0} = a_w \tag{6}$$

where p_w is the vapor pressure of water and p_w^0 is the saturation vapor pressure of water. For an aqueous solution in gas-liquid equilibrium, p_w is equal to the equilibrium water vapor pressure of a solution having a flat surface. In the case of particles, the equilibrium vapor pressure of the solution (p_{w_aerosol}) is affected by the curvature of the droplet (Kelvin effect). The magnitude of this effect is described as follows (Seinfeld and Pandis, 2006)

$$\frac{p_{w\_\text{aerosol}}}{p_w} = \exp\left(\frac{4\sigma M_w}{RT\rho_w D_p}\right) \tag{7}$$

where σ is surface tension, M_w is the molecular weight of water, R is the gas constant, T is temperature, ρ_w is the density of water, and D_p is the droplet diameter. Substituting Eq. (7) into (6), we get

$$s = \frac{p_{w\_\text{aerosol}}}{p_w^0} = a_w \exp\left(\frac{4\sigma M_w}{RT\rho_w D_p}\right) \quad (8)$$

where s is the saturation ratio of water vapor. Thus, a_w is needed to calculate s. There are several expressions for the a_w of solution. One of the most commonly used expressions is the equation defining the molal osmotic coefficient (ϕ) (Robinson and Stokes, 2002);

$$\ln a_w = -\upsilon m M_w \varphi \quad (9)$$

where υ is the stoichiometric number of solute ions and molecules, and m (molality) is defined as follows:

$$m = \frac{m_s}{M_s m_w}. \quad (10)$$

In Eq. (10), m_s is the mass of solute, M_s is molecular weight of solute, and m_w is the mass of water in aqueous solution. The van't Hoff factor (i) is also frequently used to express a_w. The value i is defined as follows:

$$a_w = \frac{n_w}{n_w + i\, n_s} \quad (11)$$

where n_w and n_i are the numbers of moles of water (solvent) and solute, respectively (Pruppacher and Klett, 1997). As an example of another expression, Tang and Munkelwitz (1994) and Tang (1996) expressed a_w as a polynomial equation with respect to the concentration of the solution (weight percent). Thermodynamics models employed for the present study are summarized in Appendix B. Among the models summarized in Appendix B, we regard that of Archer (1992) as the most reliable, as it is based on a number of experimental results, including the concentration range that is important for CCN activation (Clegg, 2007). We next derive Köhler theory using ϕ. Similar equations can easily be obtained for other expressions of a_w.

Using Eqs. (8), (9), and (10), we get

$$\ln s = \frac{4\sigma M_w}{RT\rho_w D_p} - \upsilon\varphi \frac{M_w m_s}{M_s m_w}. \quad (12)$$

In Eq. (12), we need to know m_s for the calculation of s. It is equal to m_p when the particle is composed of a single component. Then, Eq. (12) can be rewritten using d_{ve} (Eq. 1),

$$\ln s = \frac{4\sigma M_w}{RT\rho_w D_p} - \upsilon\varphi \frac{M_w \rho_m d_{ve}^3}{M_s \rho_w (D_p^3 - d_{ve}^3)} \quad (13)$$

When we calculate s of a single particle as a function of D_p, it has a maximum value. S corresponding to this value is called the critical S. If the particle is subjected to an S greater than the critical S, the particle can grow into a cloud droplet.

Table 1. M_s, ρ_m, and ν of $(NH_4)_2SO_4$ and NaCl.

	M_s (g mol^{-1})	ρ_m (g cm^{-3})	ν
$(NH_4)_2SO_4$	132.14	1.77	3
NaCl	58.44	2.16	2

3 Experiment

3.1 Particle generation and classification

The experimental setup used in this study is shown in Fig. 1. Aqueous solutions (~0.1 weight %) of $(NH_4)_2SO_4$ and NaCl were prepared and introduced into an atomizer (TSI model 3076). Chemical properties of these compounds are summarized in Table 1. Synthetic compressed air supplied from a gas cylinder was used for this atomizer. Particles were dried by passing them through two diffusion dryers (TSI model 3062) connected in tandem. Silica gel used for the diffusion dryers was regenerated before each run. Then, particles were charged with a ^{241}Am neutralizer, and their size was selected by a DMA (TSI model 3081). The sheath and sample flow rates of the DMA were set at 3.0 lpm and 0.3 lpm, respectively. The size selection of the DMA was checked by measuring size distributions of the polystyrene latex (PSL) particles listed in Table 2. The peak diameters of the size-distributions agreed with the diameters of the PSL to within the errors given by the manufacturers. In this paper, we report diameters by the set values of the DMA. The random error in diameter estimated from the PSL measurements was less than 0.5%.

3.2 CCN measurement

The CCN measurement part of Fig. 1 was used to determine the mobility equivalent critical dry diameter (d_{c_me}). A CCNC (Droplet Measurement Technologies, DMT) (Roberts and Nenes, 2005) was used to measure CCN number concentration, and a condensation particle counter (CPC: TSI model 3022) was used for CN measurement. The sample flow from the DMA was mixed with dry compressed particle-free air (0.5 lpm) to keep the sample flow rate of the DMA at 0.3 lpm. Dilution air was produced from air in the laboratory using a pure air generator (PAG 003, ECO Physics) and a high-efficiency particulate air (HEPA) filter. The flow rate of the dilution air was controlled by a mass flow controller. The sample flow and the sheath flow rates of the CCNC were set to 0.045 lpm and 0.455 lpm, respectively. Two temperature gradient (ΔT) conditions of the thermal gradient chamber inside the CCNC were used as shown in Table 3 so that the measurement was performed at two S values. Solenoid pumps used for water circulation in the CCNC were replaced by external peristaltic pumps for flow stabilization. The air

Table 2. List of PSL particles used for the calibration of the DMA and APM.

d_p (nm)	ρ_m (g cm^{-3})[a]	Mass range (fg)[b]	Manufacturer (product name)
48±1	1.061	0.058–0.065	JSR corporation (STADEX SC-0050-D)
61±1	1.065	0.12–0.13	JSR corporation (STADEX SC-0060-D)
76±2	1.057	0.22–0.26	JSR corporation (STADEX SC-0075-D)
102±3	1.05	0.53–0.64	Duke Scientific Corporation (NANOSPHERE SIZE STANDARDS)
152±5	1.05	1.7–2.1	Duke Scientific Corporation (NANOSPHERE SIZE STANDARDS)

[a] Density given by the manufacturers as a reference.
[b] Particle mass was calculated using the diameter range and density.

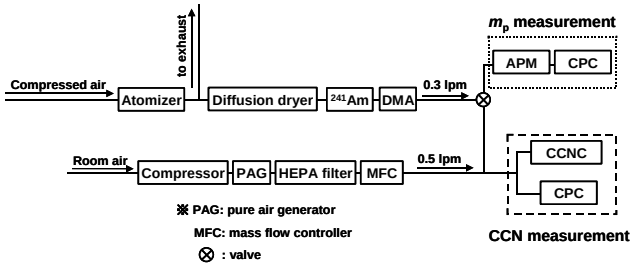

Fig. 1. Experimental setup used in this study.

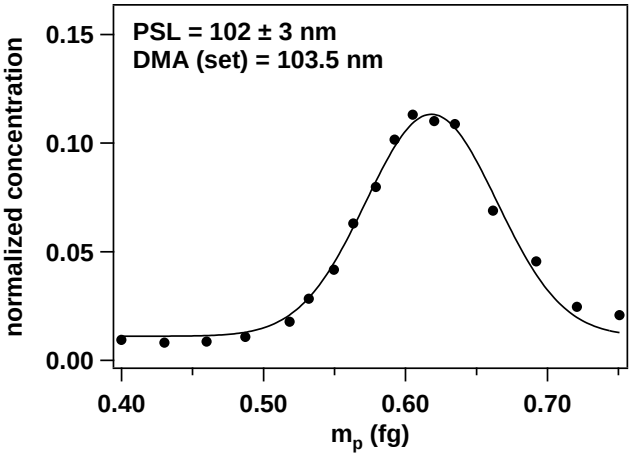

Fig. 2. Example mass distribution of PSL particles prescribed by the DMA.

circulation system for the OPC drying system was plugged to stabilize the airflow in the chamber. The reproducibility of d_{c_me} measurement was tested using $(NH_4)_2SO_4$ particles. The random errors associated with d_{c_me} measurement were 0.1 and 0.3 nm for $\Delta T1$ and $\Delta T2$, respectively. The influence of this error on the critical S was calculated to be negligibly small (less than 0.001%, absolute). Although, we employed the CCNC manufactured by DMT, the present result is applicable for other types of CCNCs, as they are calibrated similarly (e.g., Snider et al., 2006; Frank et al., 2007).

3.3 DMA-APM system

An APM (APM 302, KANOMAX JAPAN, Inc.) was employed to measure m_p of particles prescribed by the DMA. The m_p selected by the APM is described as follows (Ehara et al., 1996),

$$m_p = \frac{neV_{\mathrm{APM}}}{w^2 r^2 \ln(r_2/r_1)} \tag{14}$$

where n is the number of charges, e is the elementary charge, V_{APM} is the voltage applied to the APM, ω is the rotation speed, and r, r_1, and r_2 are the center, inner, and outer radii of the APM operating space, respectively. Particle number concentration downstream of the APM was measured by a CPC (TSI model 3022). To calibrate m_p and ρ_{eff} measurement by the DMA-APM system, the masses of DMA-selected PSL particles were measured. Figure 2 shows an example of a mass distribution of DMA-selected PSL particles. The peak of the distribution, which corresponds to m_p, was obtained by fitting the distribution by a Gaussian function. The measured values of m_p agreed with the calculated values within the errors associated with PSL particles (Table 2). Density calculated using Eqs. (14) and (1) (in this case, we can assume d_{ve}=d_{me}, as PSL particles have spherical shape) agreed with the values given by the manufacturers to within 5%, and this difference was corrected for inorganic salt particles. Linear interpolation was employed for the correction, as the difference was size-dependent. Relative contributions of the DMA and APM to the difference were not quantified. The random error associated with the ρ_{eff} measurement by the DMA-APM system was 1%, estimated from PSL measurements.

Table 3. Temperatures of the thermal gradient chamber in the CCNC. $T1$, $T2$, and $T3$ correspond to the temperatures at the top, middle, and the bottom of the chamber, respectively.

	T inlet (K)	$T1$ (K)	$T2$ (K)	$T3$ (K)
$\Delta T1$	301.3±0.1	300.48±0.02	301.86±0.02	303.16±0.02
$\Delta T2$	301.9±0.1	301.10±0.02	303.18±0.02	305.08±0.02

The measurement of ρ_{eff} was performed four times. RUN1 and RUN2 were performed prior to CCN measurement. RUN3 was performed soon after (within 5 h) the CCN measurement at $\Delta T1$, and we concentrated on the size range that is important for CCN activation under these conditions. Likewise, RUN4 was performed soon after the CCN measurement at $\Delta T2$.

4 Results and discussion

4.1 d_{c_me} of inorganic salt particles

Figure 3 shows experimental results for the CCN measurement of $(NH_4)_2SO_4$ and NaCl particles. CCN/CN ratios monotonically increase with increasing diameter and approach unity. The CCN/CN ratios are fitted by a sigmoid function (Eq. 15):

$$\frac{\text{CCN}}{\text{CN}} = a + \frac{b}{1 + \exp\left(\frac{d_{c\_me} - d_{me}}{c}\right)} \tag{15}$$

where a, b, and c are constants determined by the fitting. d_{c_me} values were 115.2 nm ($\Delta T1$) and 75.3 nm ($\Delta T2$) for $(NH_4)_2SO_4$ and 94.7 nm ($\Delta T1$) and 63.2 nm ($\Delta T2$) for NaCl, respectively.

4.2 ρ_{eff}, χ and d_{ve} of inorganic salt particles

Figure 4 shows an example mass distribution of DMA-selected NaCl particles measured using the APM and CPC. As in the case of PSL, these distributions were fitted by Gaussian functions to obtain the peak of the distribution, and then we obtained the particle mass. ρ_{eff}, d_{ve} and χ were calculated from the experimental results. The calculated values are summarized in Fig. 5. ESA was used to calculate χ in all cases, as χ_f and χ_c are not available. In the case of $(NH_4)_2SO_4$, the measured values of ρ_{eff} (1.67∼1.75 g cm^{-3}) were slightly smaller than the bulk density (1.77 g cm^{-3}) (Fig. 5a), and χ was slightly larger than unity (1.01∼1.04) (Fig. 5b). These values are similar to those obtained by Zelenyuk et al. (2006a), who showed that the χ of $(NH_4)_2SO_4$ is 1.03±0.01 at 160 nm using a DMA and a single-particle laser ablation time-of-flight mass spectrometer (SPLAT). Biskos et al. (2006a) estimated a χ for 6–60-nm $(NH_4)_2SO_4$ particles of 1.02 to explain the discrepancy between theoretical calculations and experimental results of the hygroscopicity measurement. These results indicate that $(NH_4)_2SO_4$ particles do not have a completely spherical shape, as observed by electron microscope (Dick et al., 1998; Zelenyuk et al., 2006a). Comparing the results

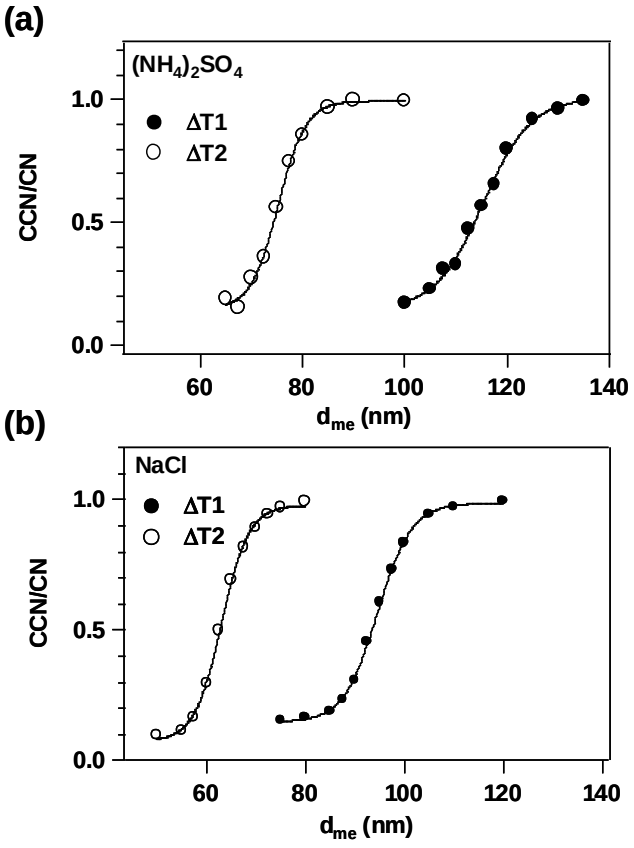

Fig. 3. CCN activation curves of $(NH_4)_2SO_4$ and NaCl particles under two experimental conditions ($\Delta T1$ and $\Delta T2$).

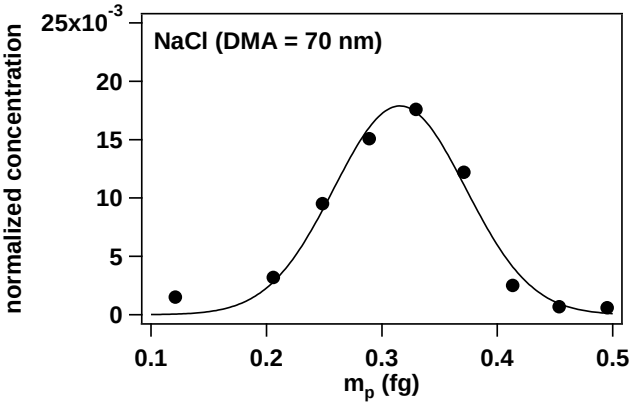

Fig. 4. Example mass distribution of NaCl particles prescribed by the DMA. The solid line is the fitting result of the experimental data to a Gaussian function.

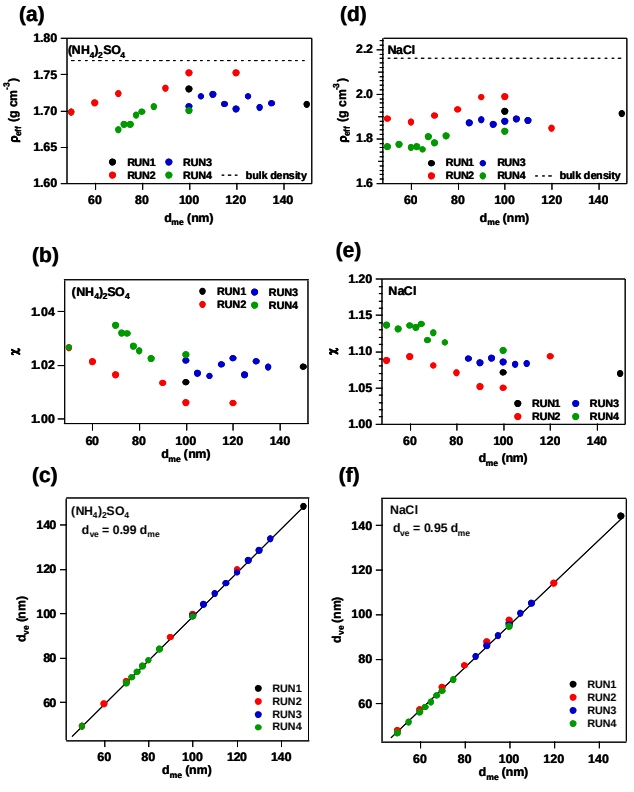

Fig. 5. ρ_{eff}, χ, and d_{ve} of $(NH_4)_2SO_4$ and NaCl particles measured using the DMA-APM system. **(a)** ρ_{eff} of $(NH_4)_2SO_4$, **(b)** χ of $(NH_4)_2SO_4$, **(c)** d_{ve} of $(NH_4)_2SO_4$, **(d)** ρ_{eff} of NaCl, **(e)** χ of NaCl, and **(f)** d_{ve} of NaCl particles.

of RUN1 ∼ RUN4, systematic differences are observed. ρ_{eff} was the highest in RUN2 and lowest in RUN4. These differences are greater than the uncertainty of the ρ_{eff} measurement (1%). Zelenyuk et al. (2006b) reported that rapid drying causes particles to have a more irregular shape. Thus, we suspect that these differences found are possibly caused by different conditions of the silica gel in the diffusion dryer in each run. Figure 5c shows the relationship between d_{me} and d_{ve} of $(NH_4)_2SO_4$ particles. As can be easily expected from the values of χ, the slope is almost equal to unity (0.99). Considering that the error in the diameter of PSL particles is typically about 3% (Table 2), this result shows that $(NH_4)_2SO_4$ particles can be treated approximately as spherical in most cases.

Figure 5d and e show ρ_{eff} and χ of NaCl particles, respectively. ρ_{eff} (1.75∼1.99 g cm^{-3}) was smaller than the bulk density (2.16 g cm^{-3}), and χ was significantly larger than unity (1.05∼1.14). Kelly and McMurry (1992) used a DMA and an impactor to measure ρ_{eff} of NaCl particles (d_{me}=111 nm). They reported that ρ_{eff} was equal to 1.86 g cm^{-3} (χ=1.08). Zelenyuk et al. (2006a) measured ρ_{eff} of NaCl (d_{me}=160∼850 nm) using a DMA and a SPLAT. They showed that ρ_{eff}∼1.95 g cm^{-3} (χ∼1.06) at 160 nm.

Table 4. Values of d_{c_ve} used for the calculation of S.

	$\Delta T1$		$\Delta T2$	
	$(NH_4)_2SO_4$	NaCl	$(NH_4)_2SO_4$	NaCl
d_{c_ve} (nm)	113.9	90.3	74.0	59.2

Mikhailov et al. (2004) estimated that χ is equal to 1.06 (99 nm) and 1.07 (201 nm) from hygroscopicity measurements. These values show that the shape of NaCl particles is significantly different from spherical. Our results shown in Fig. 5 are similar to these other studies except for RUN4. In that case, χ was systematically higher than the other cases (1.10∼1.14). This value is higher than the χ for a cubic shape in the continuous regime (1.08) (Hinds, 1999). Biskos et al. (2006b) showed that χ calculated by ASA for a cubic shape is needed to explain hygroscopic growth of d_{me}=6–60-nm NaCl particles. χ is about 1.2 for d_{me}=50–100 nm when we employ ASA to calculate the χ of cubic particles. Thus, we regard the results of RUN4 as quite reasonable, considering that the shape of NaCl particles is cubic with rounded edges (Zelenyuk et al., 2006a). Figure 5f shows the relationship between d_{me} and d_{ve} of NaCl particles. d_{ve} is smaller than d_{me} by 3–7%, and the value of the slope is 0.95. This shows that morphology should be considered when using NaCl particles for calibration experiments (Rose et al., 2008). The measurements of χ and ρ_{eff} without employing thermodynamics models are limited to the size range of <150 nm (e.g., Kelly and McMurry, 1992). Our data are also useful for the investigation of the hygroscopic growth of particles in this size range.

4.3 Calculation of *S*

In this section, we estimate S inside the CCNC using experimental results shown in Sects. 4.1 and 4.2. In order to calculate volume equivalent critical dry diameter (d_{c_ve}), d_{c_me} and ρ_{eff} at d_{c_me} are required (Eq. 1). The d_{c_me} shown in Sect. 4.1 was used, and ρ_{eff} at d_{c_me} was calculated by interpolating the corresponding experimental result of the DMA-APM system measurement (RUN3 and RUN4 for $\Delta T1$ and $\Delta T2$, respectively). The values of d_{c_ve} used for the calculation are summarized in Table 4. The calculation was performed using the temperatures at $T2$ (Table 3).

Table 5 shows the calculated results. As discussed in Sect. 2.2, we regard the model of Archer (1992) as the most reliable. Using this model, S values were calculated to be 0.117% and 0.220% for $\Delta T1$ and $\Delta T2$, respectively. Thus, we regard these values as the most probable values of S in the CCN chamber.

In the case of NaCl particles at $\Delta T1$, the value calculated using the approach of Tang (1996) was the lowest, and a higher S value was obtained with the approach of

Table 5. S values calculated using several thermodynamics models. See text for the input parameters and descriptions of the models. "N/A" denotes that the thermodynamic data is not available.

	$\Delta T1$		$\Delta T2$	
Model	$(NH_4)_2SO_4$(%)	NaCl (%)	$(NH_4)_2SO_4$(%)	NaCl (%)
Ideal solution approximation	0.110	0.115	0.207	0.214
Archer (1992)	N/A	0.117	N/A	0.220
Clegg et al. (1996)	0.117	N/A	0.225	N/A
Pitzer and Mayorga (1973)	0.117	0.117	0.225	0.220
Young and Warren (1992)	0.118	N/A	0.228	N/A
Tang and Munkelwitz (1994)	0.135	N/A	0.256	N/A
Tang (1996)	N/A	0.113	N/A	0.211
Kreidenweis et al. (2005)	0.139	0.115	0.262	0.215

Kreidenweis et al. (2005) and the ideal solution approximation. The values calculated using the Pitzer models (Pitzer and Mayorga, 1973; Archer et al., 1992) are the same. For $(NH_4)_2SO_4$ at $\Delta T1$, values similar to those of Archer (1992) were obtained when we employed the Pitzer models (Pitzer and Mayorga, 1973; Clegg et al., 1996). This indicates the validity of the Pitzer model for the calculation of S. A similar value was obtained based on the work of Young and Warren (1992). The ideal solution approximation for $(NH_4)_2SO_4$ gave the lowest S. This indicates the inappropriateness of the use of this approximation for $(NH_4)_2SO_4$. Parameterizations by Tang and Munkelwitz (1994) and Kreidenweis et al. (2005) estimated the highest values of S. These values are significantly higher than those of Archer (1992). In the case of $\Delta T2$, the trend is similar to $\Delta T1$. For NaCl particles, a_w given by Tang (1996) gave the lowest S, and the Pitzer models (Pitzer and Mayorga, 1973; Archer, 1992) gave the highest S. In the case of $(NH_4)_2SO_4$, the ideal solution approximation gave the lowest values, and the Pitzer models (Pitzer and Mayorga, 1973; Clegg et al., 1996) and that of Young and Warren (1992) gave similar values. These trends are similar to that of Rose et al. (2008). However, unlike the case of $\Delta T1$, a relatively large difference (0.005% in absolute terms) between Clegg et al. (1996) and Archer (1992) was observed at $\Delta T2$. So far, we have been unable to determine what caused this difference.

To summarize the above discussion, the Pitzer models (Pitzer and Mayorga, 1973; Archer, 1992; Clegg, 1996) are valid to estimate critical S values within an uncertainty of 2% (relative). The ideal solution approximation gives lower values of the critical S, and the parameterizations by Tang and Munkelwitz (1994) and Kreidenweis et al. (2005) yield higher values for $(NH_4)_2SO_4$. These parameterizations are based on the data of hygroscopic growth up to RH=95%. The concentration of the $(NH_4)_2SO_4$ solution at this RH is about m=1.5 mol Kg^{-1}. Figure 6 shows the ϕ of $(NH_4)_2SO_4$ given by Clegg et al. (1996). In the case of $m<1$ mol Kg^{-1}, ϕ decreases with an increase in m because

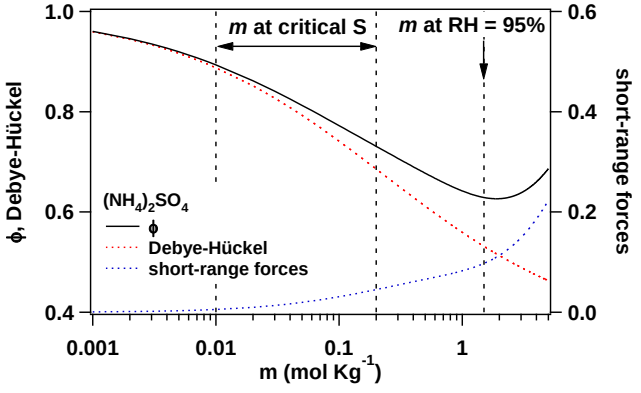

Fig. 6. ϕ and related parameters for an aqueous solution of $(NH_4)_2SO_4$ calculated based on the work of Clegg et al. (1996). "Debye-Hückel term" is the first two terms in Eq. (B2), and "short-range forces"corresponds to the third and fourth terms in the same equation.

of the Debye-Hückel effect. However, ϕ increases with the increase in m for $m>2$ mol Kg^{-1} due to short-range forces. This shows that the thermodynamic properties of $(NH_4)_2SO_4$ solutions change at around 1.5 mol Kg^{-1}. Values of m at critical S values of $(NH_4)_2SO_4$ particles were calculated to be 0.01∼0.2 mol Kg^{-1} (S=0.1∼1%), and thus the parameterizations based on a concentration range of $m>1.5$ mol Kg^{-1} are not always appropriate to calculate critical S values because they overestimate the magnitude of the non-ideality of the solution, which corresponds to an overestimation of critical S.

5 Summary and conclusion

In this study, we measured CCN/CN ratios and m_p of size-selected $(NH_4)_2SO_4$ and NaCl particles. CCN/CN ratios were measured using a CCNC and a CPC, and m_p was measured using an APM and a CPC. The CCNC was operated

under two conditions ($\Delta T1$ and $\Delta T2$). The d_{c_me} values of $(NH_4)_2SO_4$ were 115.2 nm ($\Delta T1$) and 75.3 nm ($\Delta T2$). In the case of NaCl, these values were 94.7 nm ($\Delta T1$) and 63.2 nm ($\Delta T2$). d_{ve} calculated from m_p and ρ_m were smaller than d_{me} by about 1 and 5% for $(NH_4)_2SO_4$ and NaCl, respectively. Thus, it is a good approximation to treat $(NH_4)_2SO_4$ particles as spherical particles.

d_{c_ve} values were estimated from d_{c_me} and measured ρ_{eff}, and they were used as input parameters for Köhler theory calculations. Then, S values inside the CCNC were estimated using several thermodynamics models. In these calculations, we regarded that the Pitzer model for NaCl (Archer, 1992) was the most reliable, as it was in excellent agreement with the experimental data, including the concentration range that is important for CCN activation. The values obtained for $(NH_4)_2SO_4$ and NaCl agreed to within a difference of 2% (relative) when the Pitzer model was employed for the calculation. This result indicates that application of the Pitzer model for calibrating a CCNC gives the most probable values of S.

Appendix A

List of parameters

See Table A1.

Appendix B

Thermodynamics models for a_w of inorganic salt

In this section, we review the thermodynamics models of $(NH_4)_2SO_4$ and NaCl employed in this study to estimate S in the CCNC.

B1 Ideal solution approximation

The simplest model is the ideal solution approximation (ϕ=1). Although it may be too simple (e.g., Young and Warren, 1992), this approximation has been used to calibrate CCNCs in many studies (e.g., Raymond and Pandis, 2002; Roberts and Nenes, 2005). The manufacture of CCNC also relies on this model (Shilling et al., 2007). Thus, it is important to compare this model with more sophisticated models.

B2 Pitzer model

Pitzer developed a semi-empirical model to calculate ϕ (Pitzer, 1973). Using the original Pitzer model, ϕ of a single electrolyte can be calculated by the following equation (see Appendix A for the notation of parameters):

$$\varphi = 1 - |z_m z_x| A_\phi \frac{\sqrt{I}}{1+1.2\sqrt{I}} + m\frac{2\upsilon_m\upsilon_x}{\upsilon}\left(\beta^{(0)}_{MX} + \beta^{(1)}_{MX}\exp\left(-\alpha\sqrt{I}\right)\right) + m^2\frac{(2\upsilon_m\upsilon_x)^{3/2}}{\upsilon}C^{\phi}_{MX}. \quad \text{(B1)}$$

The first two terms are derived from Debye-Hückel theory, and the third and fourth terms express short-range interactions (e.g., ion-molecular interactions). A_ϕ can be calculated as a function of temperature using the polynomial equation given by Clegg et al. (1994), which is based on the study of Archer and Wang (1990). Pitzer and Mayorga (1973) determined three parameters ($\beta^{(0)}_{MX}$, $\beta^{(1)}_{MX}$ and C^{ϕ}_{MX}) for NaCl and $(NH_4)_2SO_4$ using experimental data reviewed by Electrolyte Solutions (Robinson and Stokes, 2002). The model has been used for the calibration of CCNCs (e.g., Mochida et al., 2006) and compared with other models by Rose et al. (2008).

Archer (1991) modified Eq. (B1) as follows:

$$\varphi = 1 - |z_m z_x| A_\phi \frac{\sqrt{I}}{1+1.2\sqrt{I}} + m\frac{2\upsilon_m\upsilon_x}{\upsilon}\left(\beta^{(0)}_{MX} + \beta^{(1)}_{MX}\exp(-\alpha\sqrt{I})\right) + m^2\frac{4\upsilon_m^2\upsilon_x}{\upsilon}\left(C^{(0)}_{MX} + C^{(1)}_{MX}\exp(-\alpha_2\sqrt{I})\right) \quad \text{(B2)}$$

Archer (1992) gave the parameters of the above equation for NaCl as a function of temperature and pressure. Experimental data used by Archer (1992) cover the concentration range that is important for the calculation of critical S (on the order of 10^{-1}~10^{-2} m). Thus, we regard this model as giving the most reliable value (Clegg, 2007). Note that the correction given by Clegg et al. (1994) should be employed for the use of the work of Archer (1992). Clegg et al. (1996) obtained parameters for Eq. (B2) for $(NH_4)_2SO_4$, and their results have been used in some CCN studies (e.g., Kumar et al., 2003), and it has been compared extensively with other models by Kreidenweis et al. (2005).

B3 van't Hoff factor

Another method to express the non-ideal behavior of inorganic electrolyte solutions is the use of i. One of the most widely used expressions for i was derived by Young and Warren (1992):

$$i = 1.9242 - 0.1844\ln(\mathrm{m}) - 0.007931(\ln(\mathrm{m}))^2 \quad \text{(B3)}$$

This equation is applicable only to $(NH_4)_2SO_4$. The value from this model has been used in some studies (e.g., Svenningsson et al., 2006; Frank et al., 2007) and compared with other models by Rose et al. (2008).

B4 Polynomial equation

Tang and Munkelwitz (1994) and Tang (1996) measured hygroscopic growth of $(NH_4)_2SO_4$ and NaCl using the

Table A1. List of parameters.

Parameters	
a_i	coefficients in the polynomial equation for water density given by Kell (1975)
a_w	water activity
A_ϕ	Debye-Hückel constant for the osmotic coefficient
C_C	Cunningham slip correction factor
C_i	coefficients in the polynomial equation for water activity given by Tang and Munkelwitz (1994) and Tang (1996)
C^ϕ_{MX}, $C^{(0)}_{MX}$, $C^{(1)}_{MX}$	parameters for the Pitzer equation
d_c	critical dry diameter for CCN activation
d_{c_me}, d_{c_ve}	critical dry diameter (mobility equivalent diameter and volume equivalent diameter, respectively)
d_{me}	mobility equivalent diameter
d_{ve}	volume equivalent diameter
D_p	droplet diameter
d_p	particle diameter
e	elementary charge
I	ion strength
i	van't Hoff factor
m	molality of solution
m_p	mass of particle
m_w	mass of water
m_s	mass of solute
M_w	molecular weight of water
M_s	molecular weight of solute
n	particle charge
n_w	number of moles of water
n_s	number of moles of solute
p^0_w	saturation vapor pressure of water
p_w	equilibrium water vapor pressure of aqueous solution having a flat surface
p_{w_aerosol}	equilibrium water vapor pressure of aerosol particle
R	gas constant
r, r_1, r_2	center, inner, and outer radii of the operating space of the APM
s	saturation ratio of water vapor
S	supersaturation of water vapor
T	temperature (K)
ΔT	temperature difference along the CCNC column
V_{APM}	voltage applied to APM
x	concentration of solution in weight percent (%)
Z_p	electrical mobility
z_m, z_x	charges of ions m and x
α	a constant in the Pitzer equation
α_2	a constant in the revised Pitzer equation given by Archer (1991)
$\beta^{(0)}_{MX}$, $\beta^{(1)}_{MX}$	parameters in the Pitzer equation
λ	mean free path of air
σ	surface tension
ρ_{eff}	effective density
ρ_m	density of the material in the particle
ρ_w	density of water
υ	υ_m+υ_x (for a salt compounds written as $M\upsilon_m\ X\upsilon_x$)
υ_m, υ_x	stoichiometric number of ions m and x
ϕ	molal osmotic coefficient
ω	rotation speed of APM
χ	dynamic shape factor
χ_c, χ_t, χ_f	dynamic shape factor of continuum, transition, and free molecular regimes

electrodynamic balance (EDB) technique. They summarized the experimental results with the following polynomial function:

$$a_w = 1.0 + \sum C_i x^i \tag{B4}$$

where C_i are constants, and x is the concentration of the solution in weight %. This model has also been used to calibrate a CCNC (e.g., Snider et al., 2006) and compared with other models by Kreidenweis et al. (2005) and Rose et al. (2008).

Kreidenweis et al. (2005) fitted the growth factors (GFs) of $(NH_4)_2SO_4$ and NaCl particles measured by a hygroscopic tandem DMA with the following equation:

$$\mathrm{GF} = \frac{d_{me\_\mathrm{wet}}}{d_{me\_\mathrm{dry}}} = \left(1 + (a + ba_w + ca_w^2)\frac{a_w}{1 - a_w}\right)^{1/3} \tag{B5}$$

where a, b, and c are constants, and d_{me_wet} and d_{me_dry} denote the wet and dry particle diameters, respectively. This model has also been used for some CCN studies (e.g., Mochida et al., 2006; Rose et al., 2008).

Appendix C

ρ_w and σ

Here we summarize values of ρ_w and σ employed for the calculation of critical S. ρ_w depends both on temperature (Kell, 1975) and the concentration of solute (Tang and Munkelwitz, 1994; Tang, 1996). However, the density of the solution is available only at 25°C, and the influence of the solute on the density of solution near the critical D_p is estimated to be small. Thus, we employed the temperature-dependent water density given by Kell (1975), which is written as follows:

$$\rho_w = \frac{\sum_{i=0}^{5} a_i T^i}{1 + a_{-1} T} \tag{C1}$$

where a_i are constants.

σ also depends on temperature and chemical composition (Seinfeld and Pandis, 2006). We employed the following set of equations to calculate σ:

$$\sigma_{(NH_4)2SO_4} = \sigma_{\_\mathrm{water}}(T) + 2.17 \times 10^{-3} \mathrm{m}_{(NH_4)2SO_4} \tag{C2}$$

$$\sigma_{\mathrm{NaCl}} = \sigma_{\_\mathrm{water}}(T) + 1.62 \times 10^{-3} \mathrm{m}_{\mathrm{NaCl}} \tag{C3}$$

where

$$\sigma_{\mathrm{water}}(T) = 235.8 \times 10^{-3} \left(\frac{T_c - T}{T_c}\right)^{1.256} \left(1 - 0.625\left(\frac{T_c - T}{T_c}\right)\right) (T_c = 647.15\mathrm{K}) \tag{C4}$$

Equations (C2) and (C3) are taken from Seinfeld and Pandis (2006) and Eq. (C4) was given by Vargaftik et al. (1983).

Acknowledgements. This work was supported by the Ministry of Education, Culture, Sports, Science, and Technology (MEXT) and the global environment research fund of the Japanese Ministry of the Environment (B-083). M. Kuwata thanks to the Japan Society for the Promotion of Science (JSPS) for a JSPS Research Fellowship for Young Scientists.

Edited by: G. Roberts

References

Allen, M. D. and Raabe, O. G.: Slip correction measurements of spherical solid aerosol particles in an improved Millikan apparatus, Aerosol Sci. Tech., 4, 269–286, 1985.

Archer, D. G. and Wang, P.: The dielectric constant of water and Debye-Hückel limiting law slopes, J. Phys. Chem. Ref. Data, 19, 371–411, 1990.

Archer, D. G.: Thermodynamic properties of the NaBr + H_2O system, J. Phys. Chem. Ref. Data, 20, 509–535, 1991.

Archer, D. G.: Thermodynamic properties of the NaCl + H_2O system II. Thermodynamic properties of NaCl(aq), NaCl2H_2O(cr), and phase equilibria, J. Phys. Chem. Ref. Data, 21, 793–821, 1992.

Biskos, G., Paulsen, D., Russell, L. M., Buseck, P. R., and Martin, S. T.: Prompt deliquescence and efflorescence of aerosol nanoparticles, Atmos. Chem. Phys., 6, 4633–4642, 2006a, http://www.atmos-chem-phys.net/6/4633/2006/.

Biskos, G., Russel, L. M., Buseck, P. R., and Martin, S. T.: Nanosize effect on the hygroscopic growth factor of aerosol particles, Geophys. Res. Lett., 33, L07801, doi:10.1029/2005GL025199, 2006b.

Clegg, S. L., Rard, J. A., and Pitzer, K. S.: Thermodynamic properties of 0–6 mol Kg^{-1} aqueous sulfuric acid from 273.15 to 328.15 K, J. Chem. Soc. Faraday T., 90(13), 1875–1894, 1994.

Clegg, S. L., Milioto, S., and Palmer, D. A.: Osmotic and activity coefficients of aqueous $(NH_4)_2SO_4$ as a function of temperature, and aqueous $(NH_4)_2SO_4$-H_2SO_4 mixtures at 298.15 K and 323.15 K, J. Chem. Eng. Data, 41, 455–467, 1996.

Clegg, S. L.: Interactive comment on "Calibration and measurement uncertainties of a continuous-flow cloud condensation nuclei counter (DMT-CCNC): CCN activation of ammonium sulfate and sodium chloride aerosol particles in theory and experiments" by D. Rose et al., Atmos. Chem. Phys. Discuss., 7, S4180–S4183, 2007.

Dahneke, B. E.: Slip correction factors for nonspherical bodies-III the form of the general law, J. Aerosol Sci., 4, 163–170, 1973.

DeCarlo, P. F., Slowik, J. G., Worsnop, D. R., Davidovits, P., and Jimenez, J. L.: Particle morphology and density characterization by combining mobility and aerodynamic diameter measurements. Part 1: Theory, Aerosol Sci. Tech., 38, 1185–1205, 2004.

Dick, W. D., Ziemann, P. J., Huang, Po-Fu., and McMurry, P. H.: Optical shape fraction measurements of submicrometre laboratory and atmospheric aerosols, Meas. Sci. Technol., 9, 183–196, 1998.

Ehara, K., Hagwood, C., and Coakley, K. J.: Novel method to classify aerosol particles according to their mass-to-charge ratio-aerosol particle mass analyzer, J. Aerosol Sci., 27(2), 217–234, 1996.

Frank, G. P., Dusek, U., and Andreae, M. O.: Technical Note: Characterization of a static thermal-gradient CCN counter, Atmos. Chem. Phys., 7, 3071–3080, 2007, http://www.atmos-chem-phys.net/7/3071/2007/.

Hinds, W. C.: Aerosol Technology, John Wiley and Sons, Inc., 1999.

Kasper, G.: Dynamics and measurements of Smokes. I size characterization of nonspherical particles, Aerosol Sci. Tech., 1, 187–199, 1982.

Kell, G. S.: Precise representation of volume properties of water at one atmosphere, J. Chem. Eng. Data, 12(1), 66–69, 1967.

Kelly, W. P. and McMurry, P. H.: Measurements of particle density by inertial classification of differential mobility analyzer-generated monodisperse aerosols, Aerosol Sci. Tech., 17, 199–212, 1992.

Kreidenweis, S. M., Koehler, K., DeMott, P. J., Prenni, A. J., Carrico, C., and Ervens, B.: Water activity and activation diameters from hygroscopicity data – Part I: Theory and application to inorganic salts, Atmos. Chem. Phys., 5, 1357–1370, 2005, http://www.atmos-chem-phys.net/5/1357/2005/.

Pradeep Kumar, P., Broekhuizen, K., and Abbatt, J. P. D.: Organic acids as cloud condensation nuclei: Laboratory studies of highly soluble and insoluble species, Atmos. Chem. Phys., 3, 509–520, 2003, http://www.atmos-chem-phys.net/3/509/2003/.

Lohmann, U. and Feichter, J.: Global indirect aerosol effects: a review, Atmos. Chem. Phys., 5, 715–737, 2005, http://www.atmos-chem-phys.net/5/715/2005/.

McMurry, P. H.: A review of atmospheric aerosol measurements, Atmos. Environ., 34, 1959–1999, 2000.

Mikhailov, E., Vlasenko, S., Niessner, R., and Pöschl, U.: Interaction of aerosol particles composed of protein and saltswith water vapor: hygroscopic growth and microstructural rearrangement, Atmos. Chem. Phys., 4, 323–350, 2004, http://www.atmos-chem-phys.net/4/323/2004/.

Mochida, M., Kuwata, M., Miyakawa, T., Takegawa, N., Kawamura, K., and Kondo, Y.: Relationship between hygroscopicity and cloud condensation nuclei activity for urban aerosols in Tokyo, J. Geophys. Res., 111, D23204, doi:10.1029/2005JD006980, 2006.

Nenes, A., Chuang, P. Y., Flagan, R. C., and Seinfeld, J. H.: A theoretical analysis of cloud condensation nucleus (CCN) instruments, J. Geophys. Res., 106(D4), 3449–3474, 2001.

Otto, P., Georgii, H-W., and Bingemer H.: A new three-stage continuous flow CCN-counter, Atmos. Res., 61, 299–310, 2002.

Park, K., Kittelson, D. B., and McMurry, P. H.: Structural properties of diesel exhaust particles measured by transmission electron microscope (TEM): relationships to particle mass and mobility, Aerosol Sci. Tech., 38, 881–889, 2004.

Pitzer, K. S.: Thermodynamics of Electrolytes. I. Theoretical basis and general equations, J. Phys. Chem., 77(2), 268–277, 1973.

Pitzer, K. S. and Mayorga, G.: Thermodynamics of electrolytes. II. Activity and osmotic coefficients for strong electrolytes with one or both ions univalent, J. Phys. Chem., 77(19), 2300–2308, 1973.

Pruppacher, H. R., and Klett, J. D.: Microphysics of Clouds and Precipitation, Kluwer Academic Publishers, 1997.

Raymond, T. M. and Pandis, S. N.: Cloud activation of single-component organic aerosol particles, J. Geophys. Res., 107(D24), 4787, doi:10.1029/2002JD002159, 2002.

Rissman, T. A., Varutbangkul, V., Surratt, J. D., Topping, D. O., McFiggans, G., Flagan, R. C., and Seinfeld, J. H.: Cloud condensation nucleus (CCN) behavior of organic aerosol particles generated by atomization of water and methanol solutions, Atmos. Chem. Phys., 7, 2949–2971, 2007, http://www.atmos-chem-phys.net/7/2949/2007/.

Roberts, G. C. and Nenes, A.: A continuous-flow streamwise thermal-gradient CCN chamber for atmospheric measurements, Aerosol Sci. Tech., 39, 206–221, 2005.

Robinson, R. A. and Stokes, R. H.: Electrolyte Solutions, second revised edition, Dover Publications, Inc., 2002.

Rose, D., Gunthe, S. S., Mikhailov, E., Frank, G. P., Dusek, U., Andreae, M. O., and Pöschl, U.: Calibration and measurement uncertainties of a continuous-flow cloud condensation nuclei counter (DMT-CCNC): CCN activation of ammonium sulfate and sodium chloride aerosol particles in theory and experiment, Atmos. Chem. Phys., 8, 1153–1179, 2008, http://www.atmos-chem-phys.net/8/1153/2008/.

Seinfeld, J. H. and Pandis, S. N.: Atmospheric Chemistry and Physics, John Wiley and Sons, Inc., New York, 2006.

Shilling, J. E., King, M. E., Mochida, M., Worsnop, D. R., and Martin, S. T.: Mass spectral evidence that small changes in composition caused by oxidative aging processes alter aerosol CCN properties, J. Phys. Chem. A, 111, 3358–3368, 2007.

Snider, J. R., Petters, M. D., Wechsler, P., and Liu, P. S.: Supersaturation in the Wyoming CCN instrument, J. Atmos. Ocean. Technol., 23, 1323-1339, 2006.

Stratmann, F., Kiselev, A., Wendisch, M., Heintzenberg, J., Charlson, R. J., Diehl, K., Wex, H., and Schmidt, S.: Laboratory studies and numerical simulations of cloud droplet formation under realistic supersaturation conditions, J. Atmos. Ocean. Tech., 21, 876–887, 2004.

Svenningsson, B., Rissler, J., Swietlicki, E., Mircea, M., Bilde, M., Facchini, M. C., Decesari, S., Fuzzi, S., Zhou, J., Mønster, J., and Rosenørn, T.: Hygroscopic growth and critical supersaturations for mixed aerosol particles of inorganic and organic compounds of atmospheric relevance, Atmos. Chem. Phys., 6, 1937–1952, 2006, http://www.atmos-chem-phys.net/6/1937/2006/.

Tang, I. N. and Munkelwitz, H. R.: Water activities, densities, and refractive indices, of aqueous sulfates and sodium nitrate droplets of atmospheric importance, J. Geophys. Res., 99(D9), 18801–18808, 1994.

Tang, I. N.: Chemical and size effects of hygroscopic aerosols on light scattering coefficients, J. Geophys. Res., 101(D14), 19245–19250, 1996.

Twomey, S.: Pollution and the planetary albedo, Atmos. Environ., 8, 1251–1256, 1974.

VanReken, T. M., Ng, N. L., Flagan, R. C., and Seinfeld, J. H.: Cloud condensation nuclei activation properties of biogenic secondary organic aerosol, J. Geophys. Res., 110, D07206, doi:10.1029/2004JD005465, 2005.

Vargaftik, N. B., Volkov, B. N., and Voljak, L. D.: International tables of the surface tension of water, J. Chem. Eng. Data, 12(3), 817–820, 1983.

Young, K. C. and Warren, A. J.: A reexamination of the derivation of the equilibrium supersaturation curve for soluble particles, J. Atmos. Sci., 49(13), 1138–1143, 1992.

Zelenyuk, A., Cai, Y., and Imre D.: From agglomerates of spheres to irregularly shaped particles: determination of dynamic shape factors from measurements of mobility and vacuum aerodynamic diameter, Aerosol Sci. Technol., 40, 190-217, 2006a.

Zelenyuk, A., Imre, D., and Cuadra-Rodriguez, A. L.: Evaporation of water from particles in the aerodynamic lens inlet: an experimental study, Anal. Chem., 78, 6942–6947, 2006b.